AGU100 ADVANCING EARTH AND SPACE SCIENCE

Geophysical Research Letters

RESEARCH LETTER

10.1029/2018GL078817

Ambient Seismic Noise Image of the Structurally Controlled Heat and Fluid Feeder Pathway at Campi Flegrei Caldera

L. De Siena[1], C. Sammarco[1], D. G. Cornwell[1], M. La Rocca[2], F. Bianco[3], L. Zaccarelli[4], and H. Nakahara[5]

[1]Department of Geology and Petroleum Geology, School of Geosciences, University of Aberdeen, Aberdeen, UK, [2]Dipartimento di Biologia, Ecologia e Scienze della Terra, Università della Calabria, Rende, Italy, [3]Sezione di Napoli-Osservatorio Vesuviano, Istituto Nazionale di Geofisica e Vulcanologia, Naples, Italy, [4]Istituto Nazionale di Geofisica e Vulcanologia, Sezione di Bologna, Bologna, Italy, [5]Department of Geophysics, Graduate School of Science, Tohoku University, Sendai, Japan

Key Points:

- Rayleigh wave tomography of Campi Flegrei caldera used continuous ambient noise data recorded during the 2011–2013 volcanic unrest
- Low velocities map the aseismic pathway opened during the 1984 volcanic unrest, feeding heat and fluids to the shallow hydrothermal systems
- High-velocity intracrater domes and structural faults control the feeder extension and fluid migration to fumaroles

Supporting Information:

- Supporting Information S1

Correspondence to:
L. De Siena,
lucadesiena@abdn.ac.uk

Citation:
De Siena, L., Sammarco, C., Cornwell, D. G., La Rocca, M., Bianco, F., Zaccarelli, L., & Nakahara, H. (2018). Ambient seismic noise image of the structurally controlled heat and fluid feeder pathway at Campi Flegrei caldera. *Geophysical Research Letters*, *45*, 6428–6436. https://doi.org/10.1029/2018GL078817

Received 21 MAY 2018
Accepted 5 JUN 2018
Accepted article online 12 JUN 2018
Published online 5 JUL 2018

Abstract Earthquakes at Campi Flegrei have been low magnitude and sparse since 1985, denying onshore monitoring observations of their usual source for structural constraint: seismic tomography. Here we used continuous seismic records from 2011–2013 to reconstruct period-dependent Rayleigh wave group velocity maps of the volcano. The Neapolitan Yellow Tuff rim faults bound high-velocity intracrater products of historical eruptions, which act as a barrier for deep fluid migration. The anomaly with lowest group velocity is aseismic and corresponds to the portion of a fluid storage zone that was fractured during the 1984 volcanic unrest under Pozzuoli town. Earthquake locations show that fluids migrate from this area toward the Solfatara and Pisciarelli fumaroles along shallower low-velocity fractures. The aseismic anomaly is likely fed by a deep-seated offshore magmatic source. Its spatial relation with regional dynamics and observations from historical unrests mark the area as the most likely feeder pathway for fluid and magmatic inputs from depth.

Plain Language Summary We used the seismic noise produced by the seashore at Campi Flegrei volcano to detect magma and hot fluids under its surface. The area where likely magmatic fluids are entering the volcano was part of a reservoir, broken during the 1980s and intersected by strong earthquakes that forced the population to move outside of Pozzuoli town. This area is a *feeder pathway* as it connects deeper sources of magma, likely active since the 1980s, to the upper part of the volcano and feeds hot fluids to the hydrothermal systems. The injections of either magma or fluids that fractured the reservoir in the 1980s have changed Campi Flegrei characteristics, but the feeder pathway is still the most probable pathway for deeper magma and fluids to enter the volcano subsurface. Hazardous fluids migrate from the feeder pathway to fumaroles at Solfatara and Pisciarelli, west of the Napoli city center, following fractures and faults mapped at surface.

1. Introduction

Thousands of microearthquakes associated with strong ground deformation (e.g., Bellucci et al., 2006) and variations in geochemical gas composition (Chiodini et al., 2015) spread across Campi Flegrei caldera in 1983–1984. The seismic unrest stopped at the end of 1984 due to the opening of an ∼2-km-deep fluid reservoir, expressed as a low-velocity and high-attenuation anomaly under Pozzuoli town (Figure 1, **P**; De Siena et al., 2017; Vanorio et al., 2005). This reservoir intersected the structurally defined area of cumulative uplift between 1251 and 1536 CE (Bellucci et al., 2006; Di Vito et al., 2016) preceding the Monte Nuovo eruption (Figure 1, **M**). It was also affected by daylong seismic injections from depth throughout the 1983–1984 unrest (Figure 1, the gray polyhedron defines the injections' extent using the aperture of the corresponding seismic swarms, from De Siena et al., 2017). The injections were due to an input of likely magma and magmatic fluids (Amoruso et al., 2017) from an offshore 4-km-deep magmatic reservoir, marked by high deformation and high seismic attenuation anomaly (De Siena et al., 2017) and still active in 2011–2013 (Amoruso et al., 2014; Figure 1, the asterisk marks the center of the deformation ellipsoid). An injection on 1 April 1984 marked a drastic change in the fluid reservoir, making it subject to 2 months of aseismic slip; after this aseismic period, hundreds of microearthquakes spread from the reservoir crossing the structural faults bounding the region

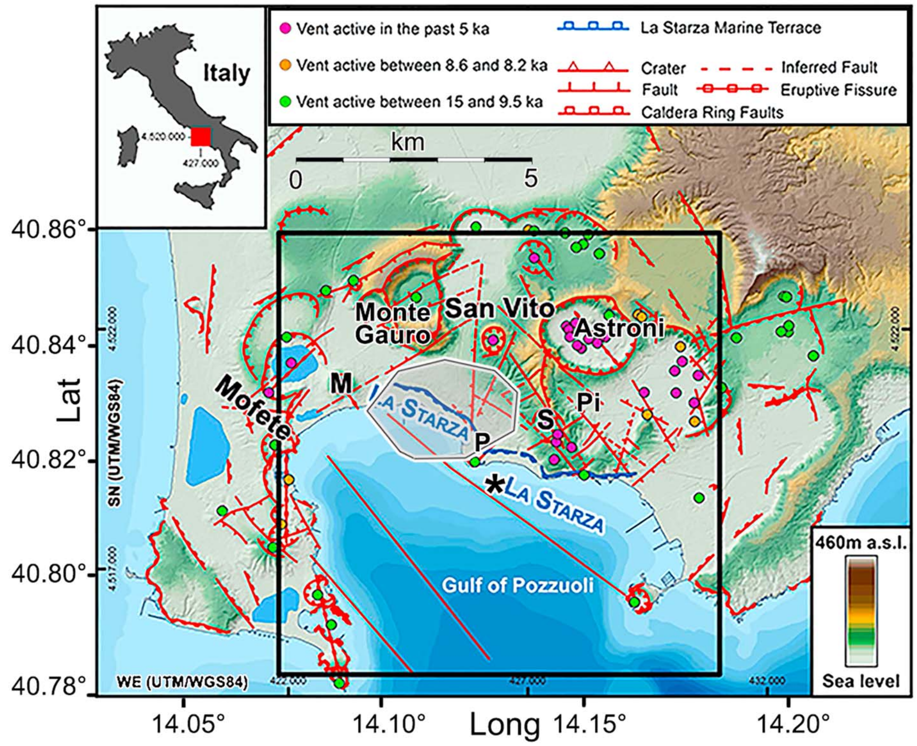

Figure 1. Structural map of Campi Flegrei caldera, redrawn from Vilardo et al. (2013) and Vitale and Isaia (2014). The upper left panel shows the caldera location in Italy. Bold letters mark the volcanic centers of Pozzuoli (**P**), Solfatara (**S**), Mt. Nuovo (**M**, and Pisciarelli (**Pi**)). The red lines are major faults and fractures. The volcanic vents are colored by age. The gray polyhedron accounts for 95% of the seismicity induced by daylong injections active throughout the 1983–1984 unrest (De Siena et al., 2017). The asterisk is the center of the main deformation anomaly modeled during the 2011–2013 unrest (Amoruso et al., 2014).

of the 1538 CE Monte Nuovo eruption (D'Auria et al., 2011; De Siena et al., 2017). Since the end of the unrest, seismicity remains low magnitude and sparse in the caldera (e.g., Di Luccio et al., 2015), while deformation and gas indicators have shown signals of volcanic unrests (Amoruso et al., 2014; Chiodini et al., 2015; Moretti et al., 2018; Trasatti et al., 2015). Some of these indicators suggest changes in the caldera's rheological characteristics (Di Luccio et al., 2015) and an approach to eruption conditions (Chiodini et al., 2016; Kilburn et al., 2017); it is thus central to understand and model both seismic structures and how earthquakes distribute on them to forecast eruptions and mitigate the related hazards.

An alternative to earthquake monitoring is to model velocity variations connected with volcanic unrest and eruptions from noise analysis (Brenguier et al., 2008). Seismic noise recorded contemporaneously at two seismic stations for a sufficient amount of time can be used to extract the fundamental mode Rayleigh wave propagating between two stations (Curtis et al., 2006). The Osservatorio Vesuviano has thus acquired and stored continuous seismic records at its temporary stations (Figure 2a, gray triangles). Since 2011, they have been used to monitor noise-derived velocity variations and, consequently, the elastic properties of the caldera (Zaccarelli & Bianco, 2017). The results of this analysis are compatible with the occurrence of a magmatic intrusion on 7 September 2012 (D'Auria et al., 2015), producing an ~2.5-km-deep seismic swarm. In 2011–2013, temporal velocity variations also correlated with geochemical (Chiodini et al., 2015, 2016) and deformation (Amoruso et al., 2014; Trasatti et al., 2015) models, showing gradual heating of the hydrothermal systems induced by a magmatic source deeper than 2 km.

Seismic imaging was used to infer if such a magmatic source existed, where it was located, and how its dynamics developed during the 1983–1984 unrest (Aster & Meyer, 1988; De Siena et al., 2017; Vanorio et al., 2005); the derived models led to an intense debate about the nature of the unrest source (fluid or magmatic) (Amoruso et al., 2014; Vanorio & Kanitpanyacharoen, 2015). Active source seismic data recorded by the SERAPIS experiment (2001) have updated the structural models of the caldera after 1984 only offshore Pozzuoli (Battaglia et al., 2008; Serlenga et al., 2016; Zollo et al., 2008). The lack of a widely distributed post-1984

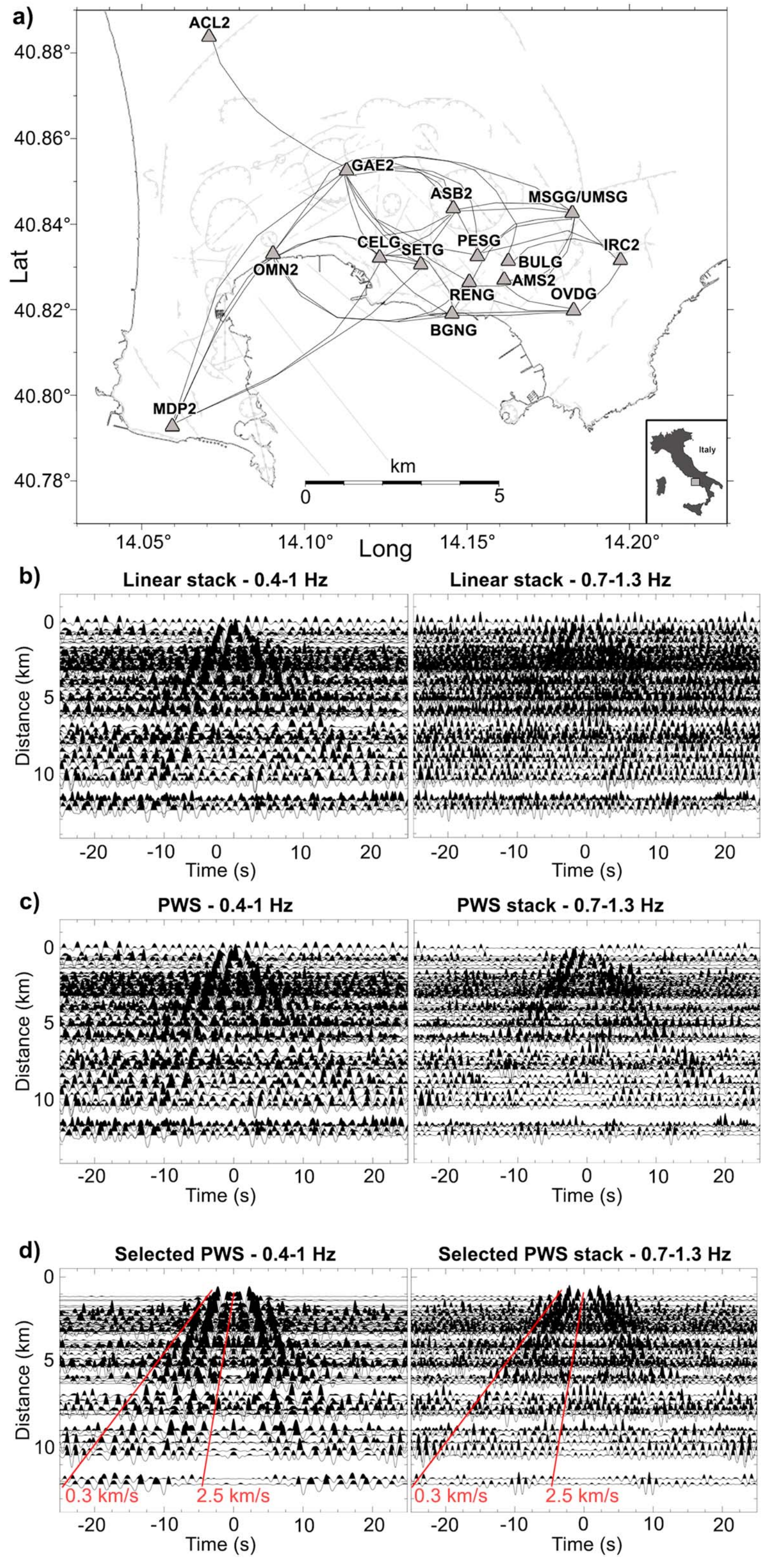

Figure 2. Seismic stations, raypaths, geomorphology, and cross correlations. (a) Seismic stations continuously recording during the 2011–2013 deformation unrest (gray triangles) are shown on the geomorphological map of Campi Flegrei caldera. The raypaths (black thin lines) are those used to produce maps at a period of 2 s. (b) Cross correlations of ambient seismic noise filtered in the two selected frequency bands using (b) linear and (c) phase-weighted stacking. (d) The stacked empirical Green's functions after the final manual selection. The red dashed lines mark the maximum and minimum velocity constraining the inversion.

seismicity precludes imaging of the onshore caldera structures, a better understanding of the post-1984 unrest dynamics, and a full assessment of the related hazards. Still, ambient seismic noise recorded between January 2011 and December 2013 can be used to track the fundamental Rayleigh mode in the caldera and perform surface wave tomography (Brenguier et al., 2007; Jaxybulatov et al., 2014). An application of this technique to the region using 3 months of noise data recorded in 2010 shows positive correlations of velocity anomalies with preexisting traveltime tomography and stratigraphy models (Costanzo et al., 2017). Here 3 years of continuous recording is used to provide the first high-resolution seismic velocity image of Campi Flegrei during a full post-1984 volcanic unrest. By mapping seismic group velocities in the shallow caldera crust, we can infer structural and unrest characteristics of the area affected by the 1983–1984 seismic injections (Figure 1, gray polyhedron), as variations in velocity anomalies are related to geological boundaries and fluid and magma contents (Brenguier et al., 2007; Jaxybulatov et al., 2014; Sammarco et al., 2017).

2. Data and Methods

We used continuous seismic recordings recorded at the temporary network of the Osservatorio Vesuviano (Figure 2a) between 2011 and 2013 (La Rocca & Galluzzo, 2015). The seismic noise processing used to obtain the cross correlations (Figure 2 and supporting information Text S1 and Figures S1 and S2) includes linear and phase-weighted stacking (Bensen et al., 2007; Schimmel & Gallart, 2007; Figures 2b and 2c). It also takes into consideration the anisotropic behavior of noise sources to improve retrieval of empirical Green's functions between 0.4 and 1.3 Hz (Figure 2d). The fundamental mode of the Rayleigh wave travels across the array with velocities of 0.3–2.5 km/s (Figure 2d, red dashed lines). We used these velocities as constraints for the inversion of the Rayleigh wave group velocities.

We apply a framework for the tomographic inversion of empirical Green's function picks for Rayleigh wave group velocities (supporting information Text S2 and Figures S3–S8) comprising frequency-time analysis for picking (Dziewonski et al., 1969; Herrmann, 2013) and the parallelized ray-dependent inversion of the Fast Marching Surface Tomography (Rawlinson & Kennett, 2008; Sammarco et al., 2017; Saygin & Kennett, 2012). We obtain group velocity maps between periods of 0.9 and 2 s (Figure 3). The velocity maps inverted with a 1-km node spacing and interpolated on a grid of 50-m step were imported into the *Voxler*© environment and overlain with available tectonic information (Isaia et al., 2009; Vilardo et al., 2013; Vitale & Isaia, 2014; Figure 3; see also Figure 1). We only interpret anomalies that are consistently recovered by the robustness and resolution tests (Figures S4–S6). We use the comparison of the results obtained with the AB and ABC data sets as robustness test (Figures S5 and S6). Due to the ray geometry, particularly at a period of 2 s (Figure 2a), and the results of the checkerboard test (Figure S4), we interpret anomalies onshore, inside, and on the Neapolitan Yellow Tuff rim (Figure 3—bright colors; see Text S2). We finally compare the velocity maps with the best localized microearthquakes nucleated in 2005–2016 (Figure 3, 2 s), obtained with a nonlinear localization technique (Lomax et al., 2001; supporting information Text S3 and Figure S9).

3. Results

We find an aseismic low-velocity structure related to infills located in the eastern part of the caldera. The structure looses definition at 2 s, while it is connected to the central low-velocity zone at 0.9 s (Figure 3). The anomaly with lowest group velocity is located between Monte Nuovo and Solfatara, NW of Pozzuoli (Figure 3, labeled **M**, **S**, and **P**, respectively) at all periods. It intersects the crossing of La Starza marine terrace with two significant SN and SSW-NNE directed faults. Particularly at a period of 2 s, the anomaly appears aseismic between 2005 and 2016, with high-velocity areas contouring it to the west, north, and east. Local faults define the boundary between low and high velocities, with background seismicity (Chiodini et al., 2017) concentrated in the first 1.5 km of the crust (Figure 3, 2 s), under the Solfatara and Pisciarelli (**Pi**, Figure 3) volcanic centers. The high-velocity zones shrink at lower periods, progressively opening low-velocity pathways toward Monte Nuovo, Solfatara, and north of Pozzuoli (Figure 3, 0.9–1.5 s). While it would be possible to obtain shear wave depth-dependent velocity maps, the significant lateral variations in velocity structures suggest the conservative approach of only analyzing group velocities. Nevertheless, considering the 1-D *S* wave velocity model used by Battaglia et al. (2008), group velocities at 2 s are sensitive to structures as deep as ~2.5 km. Figures 4a and 4b provide an interpretative sketch of the results on a map and at depth, respectively.

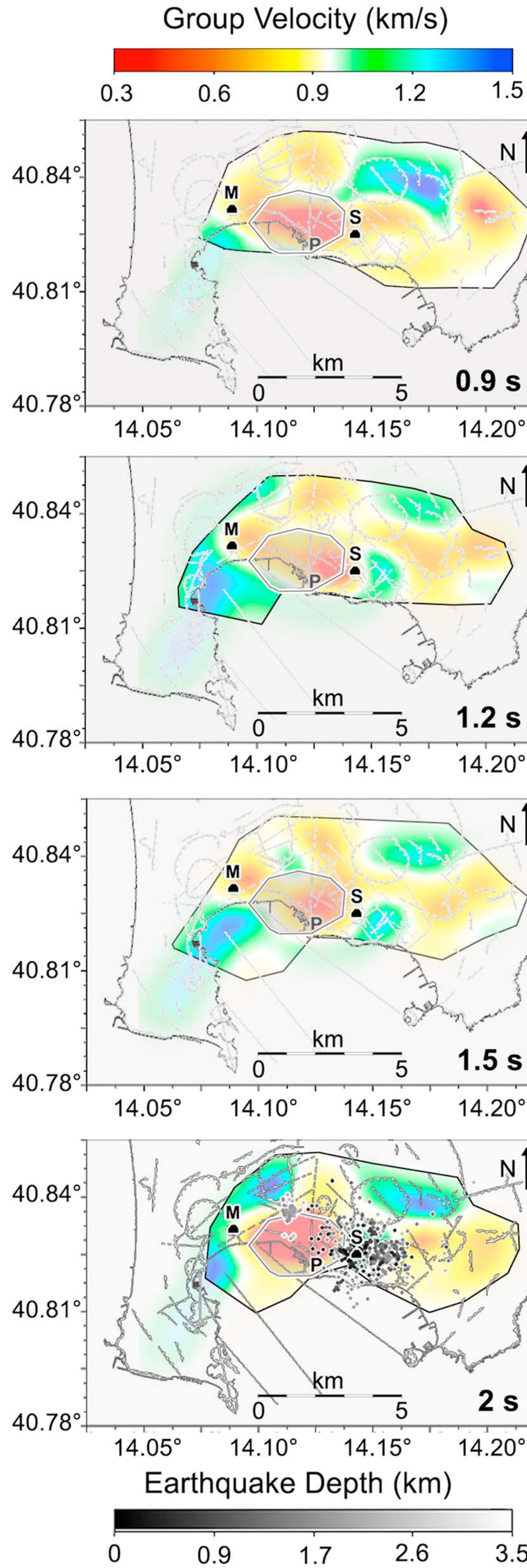

Figure 3. Ambient seismic noise-derived group velocity maps at different periods. Bold letters mark the volcanic centers of Pozzuoli (**P**), Solfatara (**S**), and Mt. Nuovo (**M**). Areas of poor or no resolution in the surface wave velocity maps are shaded following resolution and stability tests. On the 2-s panel, the gray-scaled circles show the earthquake hypocenters. The gray polyhedron overlaying all panels accounts for 95% of the seismicity induced by daylong injections active throughout the 1983–1984 unrest (De Siena et al., 2017).

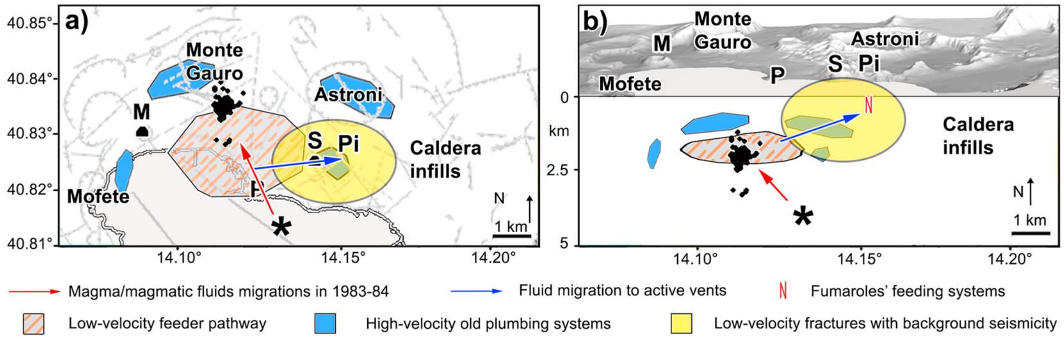

Figure 4. Map (a) and in-depth (b) sketches used to interpret the group velocity maps together with seismicity, deformation, geomorphology, and preexisting tectonic structures. Bold letters mark the volcanic centers of Pozzuoli (**P**), Solfatara (**S**), Mt. Nuovo (**M**, and Pisciarelli (**Pi**). The shaded gray-orange polyhedron and the asterisk mark the feeder pathway and the center of its magmatic source, as inferred by Amoruso et al. (2014), respectively. The arrows show the main direction of magma/magmatic fluid propagation from the deep-seated magmatic source toward the feeder pathway (red) and from the feeder pathway toward fumaroles at Solfatara and Pisciarelli (blue arrow). The yellow ellipses show the fractured low-velocity volumes intersected by the background seismicity between 2005 and 2016 (80% of total). The 7 September 2012, magmatic swarm, is reported in the figure as black circles.

4. Discussion

The area with the lowest group velocity at all periods intersects the ~2-km-deep fluid reservoir expressed as a low-velocity and high-attenuation anomaly that fed shallow hydrothermal systems in 1983–1984 (De Siena et al., 2017; Vanorio et al., 2005). At a period of 2 s, the area corresponds almost exactly to the part of the reservoir intersected by the daylong seismic injections active throughout the 1983–1984 unrest (De Siena et al., 2017; Figure 3; all panels, gray polyhedrons). As heat is increasing in the caldera systems (Chiodini et al., 2016), we interpret the area as the most likely pathway feeding fluids and heat to the shallow hydrothermal systems from depth in 2011–2013 (feeder pathway—Figure 4a, gray-orange polyhedron). The feeder pathway is mostly aseismic between 2005 and 2016 (Figure 4a) and even before, since 1985 (Di Luccio et al., 2015). In our interpretation, the cause can be traced back to an injection from depth, dated 1 April 1984. This daylong, NW directed swarm was a manifestation of a dyke intrusion and/or repeated injections of magmatic fluids from a SE high-attenuation and high-deformation source (De Siena et al., 2017), which was still active in 2011–2013 (Amoruso et al., 2014; Figures 4a and 4b; see asterisk and red arrow). The swarm drastically changed the characteristics of the feeder pathway area, making it subject to aseismic slip for almost 2 months, after which seismicity developed across the western side of the caldera (De Siena et al., 2017).

These dynamics support the view of either magma emplacement at ~3 km (Amoruso et al., 2017) or an enhancement of aseismic slip in the reservoir (De Siena et al., 2017), causing changes in the rheological characteristics of the caldera (Di Luccio et al., 2015) and, likely, the current aseismicity of the feeder pathway. The only magmatic seismic swarm detected between 2011 and 2013, nucleated on 7 September 2012 (D'Auria et al., 2015; Figure 4a, NW of Pozzuoli, black circles), confirms that a SE-to-NW regional dynamic is ongoing (Woo & Kilburn, 2010). The swarm is indeed deeper and on the opposite side of the reservoir with respect to the source of deformation, located on faults separating the Monte Gauro high-velocity anomaly from the feeder pathway (Figure 4a). The aseismicity of the reservoir and its geometry with respect to historical magmatic sources of deformation and tectonic structures (Figure 4a) hint at a central role of the feeder pathway as point of release of continuous regionally driven (Woo & Kilburn, 2010) SE-to-NW directed magmatic dynamics (e.g., Amoruso et al., 2014; Di Vito et al., 2016).

These historical and prehistorical dynamics have shaped the caldera structure and likely produced the four high-velocity structures inside the Neapolitan Yellow Tuff rim, separated from the feeder pathway by mapped faults (Figure 3, 2 s; see also Figures 4a and 4b, cyan areas). The comparison with the Campi Flegrei stratigraphy (Isaia et al., 2009) and morphometry (Vilardo et al., 2013) (see Figure 1) highlights that these structures coincide with extinct vents at Monte Gauro, Astroni, Mofete, and Solfatara (compare Figures 1 and 3, 2 s); these vents are manifestations of intracrater residuals of plumbing systems, active in the past 15 ka. In our interpretation, these high-velocity plumbing systems constrain fluid migration from the feeder pathway and play a central role in driving magmatism and fluid circulation in the shallow caldera. To assess the present hazard posed by these migration, we focus on the background shallow seismicity to the east of the reservoir (Figures 4a and 4b, yellow ellipses). Here the seismic low velocities that connect the reservoir to the eastern low-velocity caldera infills (Figures 4a and 4b, yellow ellipsoid) are compatible with the reactivation of the preexisting fractures, resulting from an increase in injection-induced pore pressure and heat (Chiodini et al., 2017; Kilburn et al., 2017). Fluids propagating from the feeder pathway are bound to travel toward Pisciarelli, where new geyser-like vents started opening in 2013 (Chiodini et al., 2015). This result supports the assessment of the eastern caldera as the zone of highest probability of vent opening (Bevilacqua et al., 2015), fed through the deeper low-velocity feeder pathway that could be identified in the group velocity maps obtained by ambient noise tomography (Figures 4a and 4b, blue arrow).

The limitations of our technique do not allow to completely remove biases produced by anisotropic noise sources (Text S2) without improving data coverage, for example, using all permanent stations and arrays storing continuous records in the same period at the caldera (Chiodini et al., 2017; La Rocca & Galluzzo, 2015). By extending data coverage and using arrays, the application of more advanced techniques like multidimensional deconvolution (Wapenaar et al., 2011) becomes feasible, likely allowing to improve modeling of absolute velocity values and characterization of the feeder pathway. The presence of degassing magma intruding the feeder pathway (e.g., D'Auria et al., 2015) cannot be assessed just by its low-velocity characteristics (Vanorio et al., 2005). Using only this marker, the area could be filled by fluids derived from hydrothermal decarbonation reactions of the basement (Vanorio & Kanitpanyacharoen, 2015). The fluids could be magmatic, produced by an ∼4-km-deep magmatic source SE of it (Amoruso et al., 2014) or by the 8-km-deep sill underlying Campi Flegrei (Moretti et al., 2018; Zollo et al., 2008). It could finally be a reservoir intruded by degassing magma, as that modeled under the urban area of Naples by deformation studies (D'Auria et al., 2015). Given the difficulty of performing active seismic experiments in the center of Pozzuoli Town, resolving the fluid/magma content in the feeder pathway would require a joint inversion with other geophysical attributes and a better integration of seismic imaging with geological and geochemical observations. We infer that magmatic fluids fill the feeder pathway with, eventually, undetectable magma sills (Amoruso et al., 2017) as this would better explain the feeder pathway's aseismicity and the shallower seismicity nucleated east of it. The stable deformation source SE of the reservoir, in this framework and driven by ongoing tectonics, was the deepest trigger of the 2011–2013 unrest (Amoruso et al., 2014). CO_2-rich fluid injections from this source may have induced thermal processes and aseismic plastic shear strain in the colder feeder pathway, which would explain the feeder pathway's aseismicity. Similar processes were observed during stimulation at the Geyser Geothermal field, United States (Jeanne et al., 2015); here they reactivated preexistent shallower fractures due to an increase in injection-induced pore pressure, causing seismicity. Such a mechanism would clarify why seismicity is shallower and only develops across the eastern side of the caldera after 1984.

5. Conclusions

Ambient seismic noise imaging is the primary available seismic imaging method at Campi Flegrei due to the absence of consistent well-spread seismicity since December 1984. The results of its application to 3 years of seismic noise data recorded during volcanic unrest (2011–2013) show that the lowest velocities are between Monte Gauro, Pozzuoli, and Monte Nuovo and cross La Starza marine terrace. The deepest low-velocity anomaly corresponds to the area fractured during the 1983–1984 unrest by NW directed seismic injections from depth, comprised in a preexistent high-pressure reservoir under Pozzuoli town. The same area is aseismic since at least 2005 and thus the most likely feeder pathway of heat and fluids from depth to the surface. Both ancient plumbing systems inside the Neapolitan Yellow Tuff rim and SE-to-NW directed tectonic structures in the caldera center constrain the feeder pathway geometry and act as a barrier for deep fluid migration. The shallow low-velocity anomalies in the eastern caldera are seismically active; this is a signature of heated hazard-prone hydrothermal systems, fed by the deeper feeder pathway, and bound to propagate toward the Pisciarelli fumarole fields via preexistent fractures and faults.

The structurally controlled feeder pathway is in spatial relation with historical preeruptive deformation records of bradyseism. Its location with respect to deformation anomalies, seismicity, and observations of historical unrests supports the existence of an ongoing NW directed feeding dynamic controlled by regional tectonics. The seismic changes affecting the low-velocity feeder pathway between 1983–1984 and 2011–2013 are evidence of its importance in controlling how and when volcanic unrests are fed. We infer that hazardous fluid and magmatic inputs from deeper magmatic sources are still likely to enter the shallower crust through the feeder pathway. During the 2011–2013 unrest, these inputs may have induced thermal processes and aseismic plastic shear strain in the colder hydrothermal reservoir associated to eastward fluid migration.

Acknowledgments
The TIDES-COST Action (STSM-ES1401-34011) provided a travel grant to framework the research project. The Japan Society for the Promotion of Science—Short-Term Fellowship (JSPS/OF215/022) financed the work, undertaken at Tohoku University and concluded at the University of Aberdeen. We thank Giuseppe Vilardo and Eliana Bellucci Sessa for providing the geomorphological maps and Simona Petrosino and Paola Cusano for the *P* and *S* wave pickings used to localize the seismicity. Informal revisions from Guido Ventura, Nick Rawlinson, and Chris Kilburn helped us improve the analyses and interpretation, respectively. We acknowledge the help of Naveed Khan in parallelizing the codes and two anonymous reviewers who improved the analysis, interpretation, and readability with their comments. All data to reproduce the maps can be downloaded from the World Data Center PANGAEA data repository, permanent link https://doi.pangaea.de/10.1594/PANGAEA.890238.

References

Amoruso, A., Crescentini, L., D'antonio, M., & Acocella, V. (2017). Thermally-assisted magma emplacement explains restless calderas. *Scientific Reports*, *7*(1), 7948.

Amoruso, A., Crescentini, L., Sabbetta, I., De Martino, P., Obrizzo, F., & Tammaro, U. (2014). Clues to the cause of the 2011–2013 Campi Flegrei caldera unrest, Italy, from continuous GPS data. *Geophysical Research Letters*, *41*, 3081–3088. https://doi.org/10.1002/2014GL059539

Aster, R., & Meyer, R. (1988). Three dimensional velocity structure and hypocenter distribution in the Campi Flegrei caldera, Italy. *Tectonophysics*, *149*, 195–218.

Battaglia, J., Zollo, A., Virieux, J., & Dello Iacono, D. (2008). Merging active and passive data sets in traveltime tomography: The case study of Campi Flegrei caldera (Southern Italy). *Geophysical Prospecting*, *56*, 555–573.

Bellucci, F., Woo, J., Kilburn, C. R., & Rolandi, G. (2006). Ground deformation at Campi Flegrei, Italy: Implications for hazard assessment. *Geological Society, London, Special Publications*, *269*(1), 141–157.

Bensen, G. D., Ritzwoller, M. H., Barmin, M. P., Levshin, A. L., Lin, F., Moschetti, M. P., et al. (2007). Processing seismic ambient noise data to obtain reliable broad-band surface wave dispersion measurements. *Geophysical Journal International*, *169*, 1239–1260.

Bevilacqua, A., Isaia, R., Neri, A., Vitale, S., Aspinall, W. P., Bisson, M., et al. (2015). Quantifying volcanic hazard at Campi Flegrei caldera (Italy) with uncertainty assessment: 1. Vent opening maps. *Journal of Geophysical Research: Solid Earth*, *120*, 2309–2329. https://doi.org/10.1002/2014JB011775

Brenguier, F., Shapiro, N. M., Campillo, M., Ferrazzini, V., Duputel, Z., Coutant, O., & Nercessian, A. (2008). Towards forecasting volcanic eruptions using seismic noise. *Nature Geoscience*, *1*, 126–130. https://doi.org/10.1038/ngeo104

Brenguier, F., Shapiro, N. M., Campillo, M., Nercessian, A., & Ferrazzini, V. (2007). 3-D surface wave tomography of the Piton de la Fournaise volcano using seismic noise correlations. *Geophysical Research Letters*, *34*, L02305. https://doi.org/10.1029/2006GL028586

Chiodini, G., Paonita, A., Aiuppa, A., Costa, A., Caliro, S., De Martino, P., et al. (2016). Magmas near the critical degassing pressure drive volcanic unrest towards a critical state. *Nature Communications*, *7*, 13712.

Chiodini, G., Selva, J., Del Pezzo, E., Marsan, D., De Siena, L., D'Auria, L., et al. (2017). Clues on the origin of post-2000 earthquakes at Campi Flegrei caldera (Italy). *Scientific Reports*, *7*, 1–10.

Chiodini, G., Vandemeulebrouck, J., Caliro, S., D'Auria, L., De Martino, P., Mangiacapra, A., & Petrillo, Z. (2015). Evidence of thermal-driven processes triggering the 2005–2014 unrest at Campi Flegrei caldera. *Earth and Planetary Science Letters*, *414*, 58–67.

Costanzo, M., Nunziata, C., & Strollo, R. (2017). Vs of the uppermost crust structure of the Campi Flegrei caldera (Southern Italy) from ambient noise rayleigh wave analysis. *Journal of Volcanology and Geothermal Research*, *347*, 278–295.

Curtis, A., Gerstoft, P., Sato, H., Snieder, R., & Wapenaar, K. (2006). Seismic interferometry: Turning noise into signal. *The Leading Edge*, *25*(9), 1082–1092.

D'Auria, L., Giudicepietro, F., Aquino, I., Borriello, G., Del Gaudio, C., Lo Bascio, D., et al. (2011). Repeated fluid-transfer episodes as a mechanism for the recent dynamics of Campi Flegrei caldera (1989–2010). *Journal of Geophysical Research*, *116*, B04313. https://doi.org/10.1029/2010JB007837

D'Auria, L., Pepe, S., Castaldo, R., Giudicepietro, F., Macedonio, G., Ricciolino, P., et al. (2015). Magma injection beneath the urban area of Naples: A new mechanism for the 2012–2013 volcanic unrest at Campi Flegrei caldera. *Scientific Reports*, *5*, 13100.

De Siena, L., Chiodini, G., Vilardo, G., Del Pezzo, E., Castellano, M., Colombelli, S., et al. (2017). Source and dynamics of a volcanic caldera unrest: Campi Flegrei, 1983–84. *Scientific Reports*, *7*, 1–13.

Di Luccio, F., Pino, N., Piscini, A., & Ventura, G. (2015). Significance of the 1982-2014 Campi Flegrei seismicity: Preexisting structures, hydrothermal processes, and hazard assessment. *Geophysical Research Letters*, *42*, 7498–7506. https://doi.org/10.1002/2015GL064962

Di Vito, M. A., Acocella, V., Aiello, G., Barra, D., Battaglia, M., Carandente, A., et al. (2016). Magma transfer at Campi Flegrei caldera (Italy) before the 1538 AD eruption. *Scientific Reports*, *6*, 32245. https://doi.org/10.1038/srep32245

Dziewonski, A., Bloch, S., & Landisman, M. (1969). A technique for the analysis of transient seismic signals. *Bulletin of the Seismological Society of America*, *59*(1), 427–444.

Herrmann, R. B. (2013). Computer programs in seismology: An evolving tool for instruction and research. *Seismological Research Letters*, *84*(6), 1081–1088.

Isaia, R., Marianelli, P., & Sbrana, A. (2009). Caldera unrest prior to intense volcanism in Campi Flegrei (Italy) at 4.0 ka B.P.: Implications for caldera dynamics and future eruptive scenarios. *Geophysical Research Letters*, *36*, L21303. https://doi.org/10.1029/2009GL040513

Jaxybulatov, K., Shapiro, N., Koulakov, I., Mordret, A., Landès, M., & Sens-Schönfelder, C. (2014). A large magmatic sill complex beneath the Toba caldera. *Science*, *346*(6209), 617–619.

Jeanne, P., Rutqvist, J., Rinaldi, A. P., Dobson, P. F., Walters, M., Hartline, C., & Garcia, J. (2015). Seismic and aseismic deformations and impact on reservoir permeability: The case of EGS stimulation at The Geysers, California, USA. *Journal of Geophysical Research: Solid Earth*, *120*, 7863–7882. https://doi.org/10.1002/2015JB012142

Kilburn, C. R. J., De Natale, G., & Carlino, S. (2017). Progressive approach to eruption at Campi Flegrei caldera in southern Italy. *Nature Communications*, *8*, 15312.

La Rocca, M., & Galluzzo, D. (2015). Seismic monitoring of Campi Flegrei and Vesuvius by stand-alone instruments. *Annals of Geophysics*, *58*(5), S0544.

Lomax, A., Zollo, A., Capuano, P., & Virieux, J. (2001). Precise, absolute earthquake location under Somma–Vesuvius volcano using a new three-dimensional velocity model. *Geophysical Journal International*, *146*, 313–331.

Moretti, R., Troise, C., Sarno, F., & De Natale, G. (2018). Caldera unrest driven by CO_2-induced drying of the deep hydrothermal system. *Scientific Reports*, *8*(1), 8309.

Rawlinson, N., & Kennett, B. (2008). Teleseismic tomography of the upper mantle beneath the southern Lachlan Orogen, Australia. *Physics of the Earth and Planetary Interiors*, *167*(1), 84–97.

Sammarco, C., Cornwell, D. G., & Rawlinson, N. (2017). Ambient noise tomography reveals basalt and sub-basalt velocity structure beneath the Faroe Islands, North Atlantic. *Tectonophysics*, *721*, 1–11.

Saygin, E., & Kennett, B. (2012). Crustal structure of Australia from ambient seismic noise tomography. *Journal of Geophysical Research*, *117*, B01304. https://doi.org/10.1029/2011JB008403

Schimmel, M., & Gallart, J. (2007). Frequency-dependent phase coherence for noise suppression in seismic array data. *Journal of Geophysical Research*, *112*, B04303. https://doi.org/10.1029/2006JB004680

Serlenga, V., Lorenzo, S., Russo, G., Amoroso, O., Garambois, S., Virieux, J., & Zollo, A. (2016). A three-dimensional Q_P imaging of the shallowest subsurface of Campi Flegrei offshore caldera, southern Italy. *Geophysical Research Letters*, *43*, 11,209–11,218. https://doi.org/10.1002/2016GL071140

Trasatti, E., Polcari, M., Bonafede, M., & Stramondo, S. (2015). Geodetic constraints to the source mechanism of the 2011–2013 unrest at Campi Flegrei (Italy) caldera. *Geophysical Research Letters*, *42*, 3847–3854. https://doi.org/10.1002/2015GL063621

Vanorio, T., & Kanitpanyacharoen, W. (2015). Rock physics of fibrous rocks akin to Roman concrete explains uplifts at Campi Flegrei Caldera. *Science*, *349*(6248), 617–621.

Vanorio, T., Virieux, J., Capuano, P., & Russo, G. (2005). Three-dimensional seismic tomography from P wave and S wave microearthquake travel times and rock physics characterization of the Campi Flegrei Caldera. *Journal of Geophysical Research*, *110*, B03201. https://doi.org/10.1029/2004JB003102

Vilardo, G., Ventura, G., Bellucci Sessa, E., & Terranova, C. (2013). Morphometry of the Campi Flegrei caldera (Southern Italy). *Journal of Maps*, *9*(4), 635–640.

Vitale, S., & Isaia, R. (2014). Fractures and faults in volcanic rocks (Campi Flegrei, southern Italy): Insight into volcano-tectonic processes. *International Journal of Earth Sciences*, *103*(3), 801–819.

Wapenaar, K., Van Der Neut, J., Ruigrok, E., Draganov, D., Hunziker, J., Slob, E., et al. (2011). Seismic interferometry by cross correlation and by multidimensional deconvolution: A systematic comparison. *Geophysical Journal International*, *185*(3), 1335–1364.

Woo, J. Y., & Kilburn, C. R. (2010). Intrusion and deformation at Campi Flegrei, southern Italy: Sills, dikes, and regional extension. *Journal of Geophysical Research*, *115*, B12210. https://doi.org/10.1029/2009JB006913

Zaccarelli, L., & Bianco, F. (2017). Noise-based seismic monitoring of the Campi Flegrei caldera. *Geophysical Research Letters*, *44*, 2237–2244. https://doi.org/10.1002/2016GL072477

Zollo, A., Maercklin, N., Vassallo, M., Dello Iacono, D., Virieux, J., & Gasparini, P. (2008). Seismic reflections reveal a massive melt layer feeding Campi Flegrei caldera. *Geophysical Research Letters*, *35*, L12306. https://doi.org/10.1029/2008GL034242